OCL 2025, 32, 28

https://doi.org/10.1051/ocl/2025021

OCL Oilseeds & fats Crops and Lipids

Available online at:
www.ocl-journal.org

RESEARCH ARTICLE OPEN ACCESS

On the difficulty of pressing hulled sunflower seeds: challenges in mechanical oil extraction☆

Florian Rousseau[1,2], Patrick Carré[2,*], Têko Gouyo[2] and Raphaëlle Savoire[1]

[1] Univ. Bordeaux, CNRS, Bordeaux INP, CBMN, UMR 5248, F-33600 Pessac, France
[2] Terres Inovia, 33600 Pessac, France

Received 26 November 2024 – Accepted 14 July 2025

Abstract – This study investigated the cold pressing of dehulled oilseeds, specifically sunflower kernels, using an instrumented continuous press at two rotational speeds (3.5 and 7 rpm). The research combined physical measurements (pressure, temperature) with oil content analysis of the cake inside the press. At 3.5 rpm, the extraction yield reached 91% with oil flow throughout the entire cage. However, at 7 rpm, the yield drastically decreased to 43%, with oil flow limited to the first half of the press. These variations corresponded to distinct pressure profiles within the press. At high speed, cake filtration resistance became limiting, leading to oil blockage due to capillary network collapse. Unidirectional compression tests revealed that increased compression speed resulted in rapid pressure rise followed by solid expulsion, which is an indicator of resistance to filtration by the dehulled product. Contrary to the most widespread hypothesis in the literature, the poor performance of screw presses with dehulled seeds is not due to lack of friction, but to increased fragility of the oil-conducting capillary network. These findings explain the poor performance of presses operating on low-fibre matrices and suggest potential improvements through adapted compression profile designs. The study also provides new insights into solid matter evolution, proposing the concept of a dominant screw segment whose flow rate determines upstream matter reflux and restricts downstream segment feeding.

Keywords: Mechanical extraction / sunflower kernels / compression speed / filtration resistance / continuous extraction

Résumé – De la difficulté de presser les amandes de tournesol : défis à relever en extraction mécanique. Cette étude a porté sur le pressage à froid d'oléagineux décortiqués, en particulier les amandes de tournesol, sur une presse continue instrumentée à deux vitesses de rotation (3,5 et 7 tr/min). La recherche a combiné des mesures physiques (pression, température) avec l'analyse de la teneur en huile du gâteau dans la presse. À 3,5 tr/min, le rendement d'extraction atteint 91% avec un écoulement d'huile sur toute la cage. À 7 tr/min, ce rendement chute à 43%, l'écoulement se limitant à la première moitié de la presse. Ces variations correspondent à des profils distincts de pression dans la presse. À vitesse élevée, la résistance à la filtration du gâteau devient limitante, provoquant un blocage de l'huile dû à l'effondrement du réseau capillaire. Des essais en compression unidirectionnelle ont montré qu'une vitesse de compression élevée entraîne une augmentation rapide de la pression suivie d'une expulsion de solide ce qui est un indicateur de la résistance à la filtration du produit décortiqué. Contrairement à l'hypothèse la plus répandue dans la littérature, les mauvaises performances des presses à vis avec les graines décortiquées ne sont pas dues à un manque de friction, mais à la fragilité du réseau capillaire permettant l'écoulement de l'huile. Ces résultats expliquent les mauvaises performances des presses sur les matrices pauvres en fibres et suggèrent des améliorations potentielles *via* la conception de profils de compression adaptés. L'étude apporte également un nouvel éclairage sur l'évolution de la phase solide, proposant le concept de segment de vis dominant dont le débit determines le reflux de matière en amont et restreint l'alimentation en aval.

Mots clés : Extraction mécanique / amandes de tournesol / vitesse de compression / résistance à la filtration / Extraction en continu

☆ Contribution to the Topical Issue: "Technological challenges in oilseed crushing and refining / Défis technologiques de la trituration et du raffinage des oléagineux".

*Corresponding author: p.carre@terresinovia.fr

Highlights

- Cold pressing of dehulled sunflower kernels studied at two screw speeds (3.5 & 7 rpm).
- High-speed pressing leads to capillary collapse and oil flow blockage.
- Pressing difficulty is linked to filtration resistance, not lack of friction.
- A new concept of a dominant screw segment is proposed to model upstream material reflux.

Abbreviations and symbols

SK Sunflower kernels
A_n Circular surface of different screw parts used to determine the volumes between the cage and the core of the screw.
V_n Volumes generated by the rotation of the worm of the "n" screw element
$\dot{M}_i$ Mass flow rate of the material *i*. (CO for crude oil, SK for sunflower kernels, 'C' for cake)
$\dot{O}_i$ Crude oil flow of segment *i*
$\dot{S}_i$ Flow rate of solid of the screw segment *i*, *i* (2, 3, 4, 5, 6)
X_j^i Concentration of the component *j* (*j* =O for oil, S for sediments) in the material *i* (*i*=CO for Crude Oil, SK for Sunflower Kernel)
SME Specific Mechanic Energy (Wh/kg)

1 Introduction

Sunflower (*Helianthus annuus L.*) is the fourth most widely grown oilseed in the world with 55.9 million tons of sunflower seeds produced worldwide in the 2023/2024 period (USDA, 2024). According to Terres Inovia (2024); sunflower seeds harvested in France have an average oil content of 45.9% and protein content of 15.7% (wet basis). Its coproduct, the sunflower meal, is an important source of proteins for livestock. It is mainly found in the form of partially dehulled meal, which has a protein content of 36.6% according to the INRAE-CIRAD-AFZ online database (Feedtables, 2024). To produce this meal, incomplete dehulling is performed, leaving approximately half of the hulls in the meal. This product therefore remains rich in fibre with 18% cellulose. The residual hulls have a limiting effect on animal growth or milk production for example (Canibe *et al.*, 1999; Park *et al.*, 1982), and reduce its economic value. By implementing complete dehulling, the meal could potentially reach a protein content of 50% and 5–7% cellulose. Nevertheless, two issues hinder the production of such meals. The first is the difficulty of dehulling modern sunflower varieties, which have been bred for high oil content at the expense of their suitability for dehulling. Addressing this obstacle falls outside the scope of this article; however, we consider that, in a facility equipped for sunflower dehulling, it remains possible to extract from the general mass a stream of well-dehulled kernels (SK) that can be directed toward higher value-added uses. The second challenge lies in the limited suitability of dehulled seeds for mechanical oil extraction, which complicates the extraction process. This limitation leads to reduced oil yields, decreased processing throughput, and a higher content of solid residues in the extracted oil.

1.1 Observations on screw presses

The challenges of pressing dehulled oilseeds in screw presses were scarcely documented before the late 20th century, with the earliest mention by Isobe *et al.* (1992). They introduced a twin-screw press for dehulled sunflower seeds, achieving a 94% extraction yield versus 20% with single-screw presses, thanks to improved pressure and prevention of cake rotation. This innovation was later adopted by a Chinese manufacturer, who developed a two-screw model (Shilong and Xiefang, 2011). Dehulling also affects subsequent oilseed processing steps like solvent extraction. Schneider and Raß (1997) noted that removing hulls from rapeseed could ease desolventization, since hexane accumulates in hull fat and is hard to remove. However, they found dehulling impractical because hulls were considered necessary for press operation. Contrary to their initial hypothesis that hulls improved cake permeability, their observations indicated that hulls hindered oil flow by their orientation. Independently, Xiao *et al.* (2005) raised a similar porosity-based explanation. Specifically, they linked the diminished extraction efficiency of dehulled rapeseed compared to whole seeds to a loss of porosity within the press cake.

To date, a single published study reports a positive impact of dehulling on extraction performance, namely the work of Lazaro *et al.* (2014). They found that dehulled sunflower seeds yielded more oil than whole seeds in a Chinese press (31–35% *vs.* 20% yield). Given initial oil contents of 44% and 60%, extraction efficiencies were low (45% and 55%), below typical screw press values, suggesting suboptimal conditions. Although the press could handle 200 kg/h, only 35 kg was processed per trial, likely preventing stable operation.

Chapuis *et al.* (2014) observed that using a OLEXA MBU 20 press, cold pressing highly dehulled Jatropha curcas kernels failed for rotation speed beyond 5 rpm. At these higher speeds, upon opening the press cage, they observed two distinct zones: a solid, hard cake near the outlet and a soft, paste-like material near the feed side with no transition between these two areas. The press blocking was due to the lack of consistency in this material, making it unsuitable for transmitting the axial thrust of the screws. A lesser rate of dehulling allowed for operation at higher rotation speeds. Similarly, Romuli *et al.* (2017) also observed that pressing dehulled Jatropha kernels was problematic. In their study using a Komet 85-2G press, pure Jatropha kernels yielded only 16% oil. However, adding 10–30% rapeseed, corn, or soybean seeds significantly improved extraction, with soybean being the most effective (yielding up to 91%). These improvements were attributed to the additives increasing friction and resistance within the press, thereby enhancing extraction efficiency. Another similar conclusion is found in Zheng *et al.* (2003). Studying screw pressing of dehulled flaxseed with a Komet S87G, they observed that it yielded less oil than whole seeds. They attributed this to the dehulled seeds' softer texture and lower fibre content, which reduced friction in the press and required a special screw configuration This was also observed by an Indian team in a series of studies (Mridula *et al.*, 2015, 2019, 2020a, 2020b) using a Komet 59G press on dehulled flaxseed, peanuts, and sunflower, each mixed with different fibre sources. Regardless of the seed or fibre used, adding fibres consistently improved oil yield, an effect attributed to increased friction.

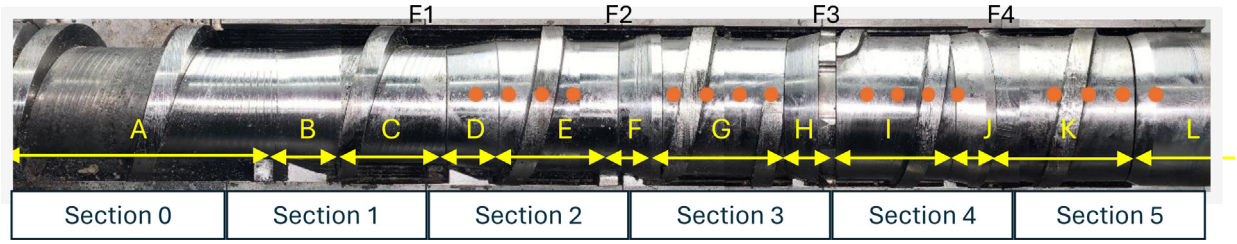

Fig. 1. Picture of the worm assembly with the knives. The orange dots represent the position of the pressure sensors. The markers F1, F2, F3, and F4 indicate the position of clamping rings equipped with strain sensors – sections are the bar sections where oil flow rates were measured.

Table 1. Geometric information about the screw

Segment	*A*	*B*	*C*	*D*	*E*	*F*	*G*	*H*	*I*	*J*	*K*	*L*
Inlet diameter (mm)	68	*68*	73	*73*	81.5	*81.5*	84	*84*	86	*86*	89	89
Outlet diameter (mm)	68	*73*	73	*81.5*	81.5	*89*	84	*91*	86	*95*	89	93.5
Length (mm)	152	38	65	30	75	25	75	30	70	25	85	110
Rotation of the thread (°)	716		284		396		446		401		536	
Pitch of the screw (mm)	70		50		45		40		40		40	
Volume / rev (cm^3) Eq.1	295		191		119		99		88		72	
Compression ratio Eq. 2&3		*1.14*	1.54	*1.37*	1.61	*1.56*	1.20	*1.64*	1.21	*2.38*	1.23	1.56

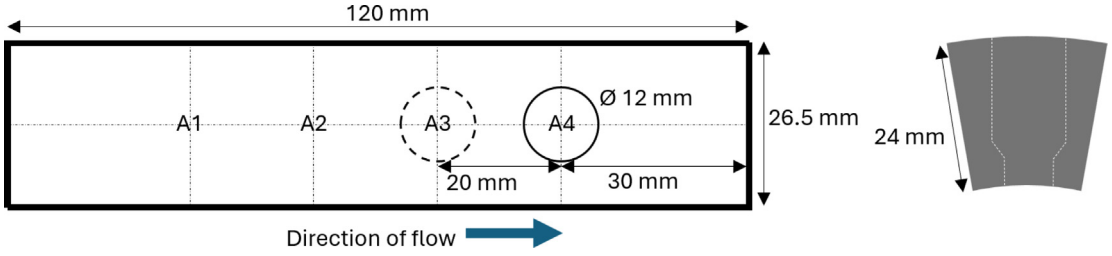

Fig. 2. Dimensions of bar supporting the pressure sensors. Left side: view from the outside of the cage, on the right side, profile view. The dotted circle indicates alternative position available for the sensor; A1, A2, A3 and A4 indicate the possible positioning of the sensors depending on the bar and its orientation. These bars are positioned in sections 2 to 5 of the cage (Fig. 1).

In addition to previous hypotheses regarding the challenges of mechanically extracting oil from dehulled materials, Carré (2022) suggested that hulls play a key role in determining the rheology of the press cake. According to this view, hulls increase the material's resistance to compression, enabling the screw to generate higher pressure. When hulls are removed, the cake becomes more plastic and softer, allowing it to pass through the press restrictive elements more easily but without building sufficient pressure to efficiently extract the oil.

1.2 Observations on unidirectional presses

Bogaert *et al.* (2018) investigated the impact of hulls in an unidirectional compression system (piston press). Using a constant pressure of 100 bar, they found that dehulling decreased oil extraction efficiency. They attributed the effect of the hull to the enhancement of the drainage capacity of the canola press-cake.

Raβ's thesis (2001) presents the most thorough analysis of unidirectional mechanical extraction from rapeseed kernels. His experimental setup enabled precise differentiation between piston force and liquid pressure in the compression chamber, using a base-mounted pressure sensor, and allowed for oil injection to assess percolation speed while the piston remained stationary. Relaxation tests, in which the piston was paused for set intervals, provided further insight into changes in cake force and liquid pressure. Raβ found that decreasing hull content led to a more rapid increase in liquid pressure compared to hulled samples. During relaxation phases, oil evacuation reduced the pressure required when compression resumed. The presence of hulls, randomly distributed among kernel particles, was shown to be crucial for stabilizing capillaries during compression; without hulls, the capillary network became fragile, resulting in a rapid increase in filtration resistance. Additionally, compression speed significantly influenced the onset of exponential increases in liquid pressure. The relaxation phase was marked by rapid redistribution of liquid, drainage toward the press exterior, and deformation of solid particles, which tended to occupy spaces left by the displaced oil.

1.3 Approach and objectives of this study

All these studies confirm the negative effect of dehulling on press performance. Regardless of the seed studied, apart from Lazaro *et al.* (2014), experimenters observe a degradation in mechanical extraction performance. However, the explanations put forward to explain this phenomenon are less unanimous. Work carried out on screw presses generally invokes a loss of friction, while work on piston presses tends to invoke a loss of filtration capacity. In fact, it is logical that devices using piston presses cannot observe a friction effect because in this device the cake does not have the ability to exit the compression chamber, whereas as Carré (2022) explains, in screw presses, the cake's resistance to thrust is necessary for pressure generation. What is commonly referred to as friction could be, in fact, more accurately described as the material's resistance to deformation.

The objective of this work was to continue elucidating the phenomena responsible for the poor performance of screw presses in extracting dehulled seeds at low temperature. It constitutes a preliminary step towards modelling the operation of presses with a view to improve compression profiles for better extraction yields at moderate temperature.

2 Materials and methods

2.1 Raw materials

Fully dehulled sunflower seeds were purchased from Flanquard, France. These oil-rich confectionery seeds, intended for human consumption, are derived from large, striated seeds. Dehulled seed oil content was 57.3% (measured according to NF V03 908 standard) and moisture content 4.6% (NF V03 909).

2.2 Instrumented screw press

The instrumented screw press is a MBU20 (Olexa, France) modified for the installation of pressure sensors. The press is equipped with a 7 kW asynchronous motor controlled by a frequency inverter (Altivar Process ATV900, Schneider Electric, France). The gearbox ensures a rotational speed of 17.5 rpm at 50 Hz when the press is empty. Rotational speed is proportional to frequency; however, because the motor is asynchronous, slip occurs as the press workload increases. The rotational speeds reported here were determined from the duration of the signal fluctuations.

2.2.1 Arrangement and instrumentation

The cage has a length of 760 mm, its constant internal diameter measures 101 mm from the entrance to the exit. The worm assembly is 730 mm long. Figure 1 presents its profile and Table 1 gives its geometrical characteristics. It can be described as a succession of worm segments separated by conical rings. A serrated disk located at 510 mm from the start separates the fourth conical ring from the fifth segment of worm. The cage is formed of two heavy frames supporting six sections of 24 lining bars (or bars) by means of semi-circular hoops (clamping rings). The frames are held by seventeen large bolts to form a cylindrical barrel enclosing the worm assembly. The bars that hold the bars have protrusions towards the internal area of the cage at the level of the conical rings, known as knives. The role of these knives is to prevent the cake from rotating with the screw. The bars have a rectangular shape of 24 x 120 mm and a thickness of 5 mm. The gap separating these bars is controlled by spacers, thin metal sheet pieces of known thickness, cut to fit between the bars at the level of the hoops without protruding more than a few tenths of a millimetre into the internal cavity of the cage. The spacing evolves depending on the cage' section (0.5 mm for the sections 0 and 1 – feeding area, 0.4 mm in section 2, 0.3 mm in section 3, 0.2 mm in section 4 and 0.1 mm in ection 5). At the screw outlet, a sliding conical ring is mounted on the shaft. Its diameter increases in the direction of the cake flow. It allows control of the cake thickness by closing the annular space between this ring and the fixed ring that terminates the cage. Its position is adjusted by tightening a nut at the end of the shaft. The purpose of this obturator is to create an additional restriction at the cake outlet in order to generate more pressure. Pressure and temperature are measured on the last four sections of the cage using respectively PL5400 (0-400 bar radial pressure, IFM, France) pressure transducer and 2 mm PT 100 probes (TCSA, France). The sensors are fixed on enlarged bars located in the middle of the cage *i.e.* at 90° from the vertical axis. Four pressure transducers and six temperature probes are used simultaneously. These modified bars are available in two versions differing by the position of the pressure sensor (Figure 2), 30 mm from the extremity for one, 50 mm for the other. By flipping the orientation of this bar, it is possible to change the location of the sensor by 20 mm intervals for each cage section hereinafter referred to as positions A1, A2, A3 and A4. The first possible position is 250 mm from the start of the worm assembly. It is not possible to position these pressure sensors at the place of the clamping rings, therefore there is a gap of 60 mm between each section where no pressure measurement is available. Temperature sensors are placed into a blind hole on the same barrels as the pressure sensor.

Between the gearbox and the screw is the thrust bearing that allows the transfer of axial thrust generated by the rotation of the screw to the cage and prevents the shaft from moving backwards. Between the thrust housing and the cage, a 200 kN annular force sensor (PM Instrumentation Model LWPF2) is placed to measure the thrust force. Four of the clamping rings (referred F1 to F4) are equipped with strain gauge (HBK 1-XY31-3/350), providing additional information on the outward pressure exerted by measure of the strain of the clamping rings with an accuracy of 1µm in two orthogonal directions. The screw segments and conical rings forming the worm assembly are labelled with letter A to L, as shown in several figures throughout this article and in Table 1. This Table presents the dimensional characteristics of each of these screw parts with indication of the compression rates. The values regarding the conical rings are expressing the difference in surface area between the entrance to the ring and the exit (Eq. (3)). For example, the 'B' ring starts at a 68 mm diameter and finishes at 73 mm, thus, the input area is delimited by two concentric circles of 101 and 68 mm, *i.e.* an area of 4380 mm² and the output side by circles of 101 and 73 mm, *i.e.* 3826 mm². To pass through this conical ring, the material must undergo a 14% strain. This strain is a combination of volume reduction and an increase in axial displacement speed, which depends on

the available volume downstream of the cone. The rate of compression mentioned for the screw sections compares the volumes generated by the rotation of the screw with the one of the preceding screw segments (Eqs. (1) and (2)). For example, with the segment 'C', the volume generated by the rotation of the upstream screw is 295 cm^3 while it is 191 cm^3 for the 'C' screw, therefore compression rate = 294/191 = 1.54.

$$\text{Volume}V_n = (A_1 - A_n)\,\text{x Pitch}, \tag{1}$$

$$\text{Compression rate screw n} = V_{n-1}/V_n, \tag{2}$$

$$\text{Compression rate for conical ring n} = (A_1 - A_o)/(A_1 - A_i), \tag{3}$$

with V_n = volume of the screw n; A_1 = area of the cage section; A_n = core area of screw; A_o = area of the outlet of ring cone; A_i = area of the inlet of ring cone.

2.2.2 Operating procedures

The study aimed at comparing the functioning of the press at two rotation speeds. The frequency setpoints given to the inverter were 10 Hz for the lowest speed and 20 Hz for the highest (3.5 rpm and 7.0 rpm respectively at screw level). Before each experiment, the press was cleaned by opening the cage and removing the cakes residues left after stopping the rotation. Before reaching the steady phase, the press was operated with rapeseed for sixty minutes at 10 Hz, followed by thirty minutes at 20 Hz, to stabilize the cage temperature in the last bars section at 57 °C. It was then operated at 10 Hz with SK for thirty minutes. Subsequently, the frequency was set to 20 Hz with rapeseed for another thirty minutes, before a final observational period of twenty minutes with SK. Choke opening was adjusted to 1.2 mm by tightening the nut controlling the position of the obturator and measuring the thickness of the cake with a caliper. The press was fed by gravity with kernels at room temperature. The first screw in the feeding area was maintained full during all the duration of the experiment. Each observation was repeated 3 times.

The crude oil collected contained solid impurities in variable amounts requiring a determination of the sediments content of these crude oils.

2.2.3 Sampling and observations

2.2.3.1 Oil and cake flow rates

Flow rate measurements were carried out by collecting samples of oil and cake for 60 seconds and repeating the measurement three times under stabilized conditions. Oil flows were collected below the 5 cage sections shown in Figure 1, using 100 mm wide boxes corresponding to the free length of the bars between the clamping rings. After collection, oils and cakes were weighed on a 10^{-2} g precision scale. The sunflower kernel input rate was determined by recording the time required to process 25 kg of kernels.

Several methods are possible for measuring oil yields. The most straightforward method involves calculating the ratio of the oil flow collected beneath the cage to the oil content of the kernels as in equation (4)

$$Yield\,(1) = \frac{\dot{M}_{CO}}{\dot{M}_{SK}.X_o^{SK}} \tag{4}$$

with $\dot{M}_{CO}$ = flow of crude oil (kg/h); $\dot{M}_{SK}$ = flow of sunflower kernels (kg/h); X_o^{SK} = oil content in sunflower kernels (%).

This initial method does not account for the presence of sediments in the collected oil; nevertheless, it provides a readily calculable first approximation, allowing for a rough comparison of flow evolution in the absence of more precise data on the composition of press cakes and crude oils. When a rapid method for evaluating the oil content of press cakes is available, as in our case using Nuclear Magnetic Resonance, a second possible approach involves considering all oil not contained in the press cakes as extracted oil. The yield is then expressed using equation (5).

$$Yield(2) = \frac{\dot{M}_{SK}.X_o^{SK} - \dot{M}_C.X_o^C}{\dot{M}_{SK}.X_o^{SK}} \tag{5}$$

With $\dot{M}_C$ = flow of cake output (kg/h); X_o^C = oil content in cake (%).

This method has the disadvantage of not considering the oil remaining in the sediments, which assumes that the sediments are fully recycled back to the press. However, the recycling of sediments impacts the operation of the presses, potentially negatively affecting their extraction efficiency, especially when sediments represent a significant portion of the oil flow (Uitterhaegen and Evon, 2017). Nevertheless, establishing a stabilized sediment recycling process would have been challenging due to the time required for such operations. Most studies conducted by our predecessors under similar conditions also did not have the opportunity to implement such recycling (see, for example, Vadke *et al.*, 1988; Bogaert *et al.*, 2018). A third method considers the ratio of clarified oil flow to the oil flux contained in the seed kernels, expressed by equation (6).

$$Yield\,(3) = \frac{\dot{M}_{CO}.(1 - X_S^{CO})}{\dot{M}_{SK}.X_o^{SK}} \tag{6}$$

With X_S^{CO} = sediment concentration in crude oil (%); $\dot{M}_{CO}$ = flow of crude oil in kg/h.

This latter method reflects the yield of clarified oil and does not account for sediment recycling. Consequently, it underestimates the potential yield but provides a more accurate representation of the actual pressing efficiency compared to the first method. A comparison between the second and third yield calculations offers a more comprehensive understanding of the process efficiency.

2.2.4 Measurement of the oil content evolution in the cake inside the press

At the end of the observation period, the press was abruptly stopped while fully loaded, and the cage was quickly and carefully opened to collect a series of cake samples. Samples were collected from the point where visible compression of the SK could be observed up to the press outlet. To track the

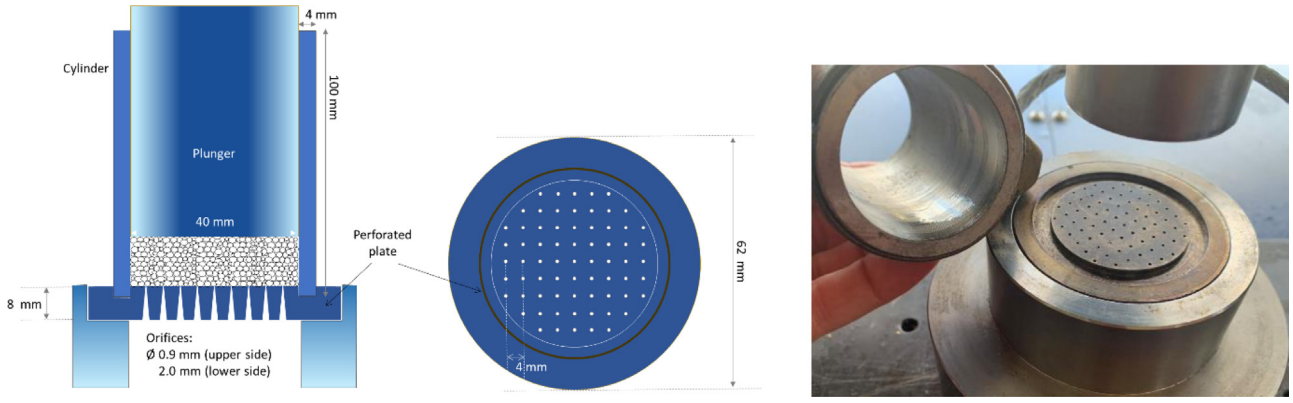

Fig. 3. Diagram and picture of the unidirectional press (compression chamber).

evolution of oil content in relation to the screw geometry, sampling was performed at 20 mm intervals each yielding approximately 10 grams of material.

2.2.5 Samples characterization

2.2.5.1 Determination of oil sediment content

The oil samples collected during mass flow rate measurements were placed in jars and shaken by hand, before pouring 15 mL in 25 mL Falcon tubes. Sediment content of the oil was determined by centrifugation at 14 000 G for 12 min (Rotanta 460 RF, Hettich, Germany). After centrifugation the supernatant was removed using a Pasteur pipette, and the residual oil was removed by gravity, the test tube being inverted for exactly 20 seconds to allow the residual oil to drain. The test tube was weighed empty, before centrifugation and after clarified oil removal for pellet mass determination with a precision of 0.01 g.

The sediment content was calculated according to equation (7).

$$X_S^{CO} = \frac{M_i - M_p}{M_i}, \tag{7}$$

with X_S^{CO} = sediment concentration in crude oil (%), M_i = initial mass of crude oil in the tube (g), M_p = mass of the pellet (g).

2.2.5.2 Determination of oil content

The residual oil content of the cakes samples has been measured using solid state NMR following the ISO 10632 standard. The NMR was a low-resolution Minispec 10 NMR from Brucker. The standard is calibrated internally.

2.3 Unidirectional press

The unidirectional press used a universal testing machine (Omnitest 50, Mecmesin, United-Kingdom, 50 kN force sensor). The compression module was specifically fabricated for studying the compressibility of oilseeds. The entire setup is illustrated in Figure 3.

The module consists of four main components. A hollow vertical cylinder with an internal cavity diameter of 40.05 mm and wall thickness of 4 mm forms the primary structure. This cylinder rests on a metal disc, which has been machined to a depth of 1.5 mm to accommodate the cylinder and ensure compression chamber sealing. The disc, 8 mm in thickness, is perforated with 69 through-holes. These perforations have a diameter of 0.9 mm on the compression chamber side and are conically shaped, measuring 2 mm in diameter at the base. The perforations are evenly distributed across the entire disc surface. This shape and diameter of holes were chosen to avoid a too easy or too hard extrusion of solid materials through the holes. The third component is a piston (plunger), which is a cylinder with a diameter of 39.95 mm, machined to slide easily within the compression chamber. This piston is connected to the force sensor and the mobile stand of the Mecmesin tester. The final component is the base, a large metal piece that supports the perforated disc. This base is equipped with a receptacle designed to collect the oil that passes through the perforated plate. With a surface area of 12.57 cm², the piston at 50 kN delivers a pressure of 398 bar. The tests on SK were performed at room temperature (25 °C). The system is controlled by a computer using the VectorPro software (Mecmesin, UK). It controls the piston displacement while simultaneously recording its position and the applied force at a frequency of 50 measurements per second. In the frame of this work, it operated at constant speed. Knowing the initial height of the sample, it is possible to trace strain (rate of deformation) versus stress curves.

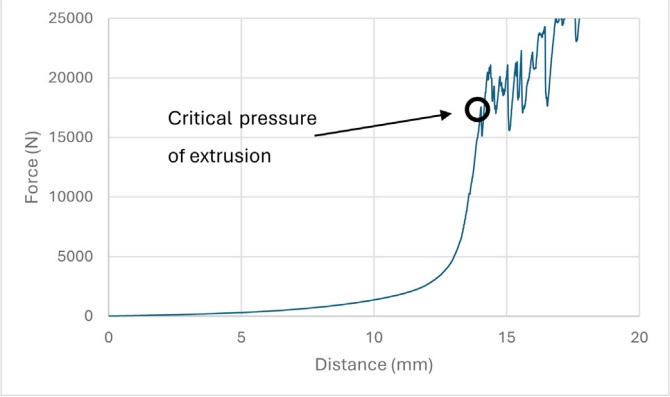

Fig. 4. Manifestation of solid material extrusion from unidirectional press on the compression curve (serration effect.)

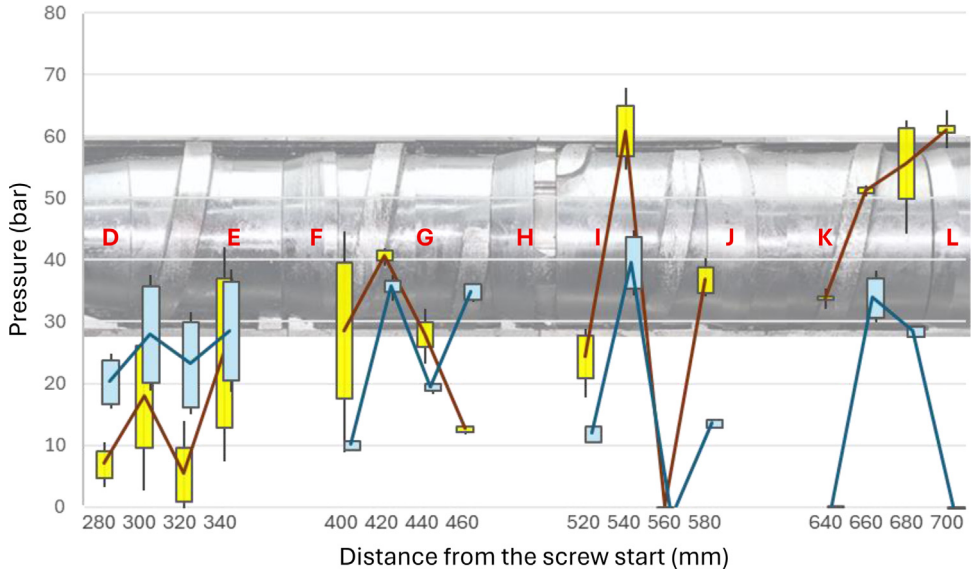

Fig. 5. Representation of the pressures measured at 16 locations on the cage at 7 rpm (blue lines and boxes) and 3.5 rpm (brown line, yellow boxes) in the processing of sunflower kernels. The boxes present average minimal and maximal pressure, the whiskers the standard deviation of these data. Broken lines join the midpoint between these values.

It is common practice to use filters between the perforated plate and the sample to prevent loss of solid material (Savoire *et al.*, 2013). However, this phenomenon is itself indicative of matrix behaviour under compression since the mechanical extraction of oil is a process of solid-liquid separation which must contend with the solid material strain. Therefore, in the context of this work, the compression chamber was used without these filters. The extrusion of solid material through the press' orifices described as a "serration effects" has been reported for the first time by Divišová *et al.* (2014) and has been observed in subsequent works of the same team (Sigalingging *et al.*, 2015; Kabutey *et al.*, 2015; Demirel *et al.*, 2017). This serration effect is the consequence of the expulsion of solid material through the press filtering plate. It manifests on the compression curves as a change in the curve's evolution during a phase of rapid force increase, which is characterized by serrations as shown in Figure 4.

The circled point on the curve represents the force at which extrusion starts happening. It was called the critical pressure of extrusion in this work. Its apparition was studied at room temperature for compression speeds ranging from 1 mm/min to 20 mm/min.

3 Results

3.1 Continuous extraction on the experimental screw press

3.1.1 Measures of the pressure on the screw press

Figure 5 represents the concatenation of the pressure measurements made on the cage for each position of the sensors (see Fig. 2). The boxes are delimited by the average maximum and minimum pressures measured at a single point. The lines extending from the boxes represent the standard deviation of these pressure measurements. The broken line passing through the centre of the boxes represents the evolution of the median pressure point. Table 2 summarizes these values.

Table 2. Pressure sensor data: Mean values of midpoints and amplitudes ranges for positions A1 through A4 at rotational speeds of 3.5 and 7 rpm. P 1- 280-340 mm distance from the screw start, P2 – 400-460 mm, P3- 520-580 mm and P4 – 640-700 mm

Pressures (bar)			P1	P2	P3	P4
Midpoint	3.5 rpm	A1	6.8	28.5	24.3	33.8
		A2	17.8	40.7	60.9	51.2
		A3	5.2	27.9	-0.3	55.6
		A4	24.9	12.6	36.7	61.2
	7 rpm	A1	20.5	10.2	12.0	0.3
		A2	28.2	36.0	39.8	34.1
		A3	23.3	19.6	-1.7	28.6
		A4	28.7	35.0	13.7	0.1
Amplitudes	3.5 rpm	A1	4.5	21.9	6.9	0.5
		A2	16.5	1.8	8.1	0.9
		A3	8.7	4.1	0.1	11.5
		A4	24.2	0.9	4.1	1.0
	7 rpm	A1	7.2	1.5	2.5	0.1
		A2	15.6	1.8	8.2	6.3
		A3	13.9	1.2	0.4	1.5
		A4	16.1	2.5	1.1	0.1

To avoid overlap of the data figures, the boxes for the 7 rpm series were slightly offset to the right. The midpoint is the medium point between the maximum and the minimum value of pressure, and the amplitude is the delta between the maximum and minimum pressure values.

Further details on pressure measurement are available in a second article (Carré *et al.* 2025).

Table 3. Throughputs measures, oil yields assessment, pressure, power and temperature (Pressure sensors in position A1).

Speed (rpm)		3.5 rpm	7 rpm
SK input	kg/h	22.75 ± *0.23*	39.33 ± *0.17*
Cake output	kg/h	10.84 ± *0.34*	29.71 ± *0.15*
Oil output	kg/h	11.91 ± *0.08*	9.62 ± *0.06*
Clarified oil output	kg/h	9.77 ± *0.07*	7.42 ± *0.05*
Foots output	kg/h	2.14 ± *0.02*	2.19 ± *0.01*
Oil yield (1)		91.4% ± *1.35%*	42.7% ± *0.25%*
Oil yield (2)		92.8% ± *0.25%*	43.8% ± *2.76%*
Oil yield (3)		75.0% ± *1.11%*	35.0% ± *0.21%*
Residual oil / cake	(%)	8.63 ± *0.18*	42.60 ± *2.12*
Crude Oil	g/rev.	56.72 ± *0.40*	22.90 ± *0.14*
Clarified oil output	g/rev.	41.34 ± *1.95*	15.47 ± *0.09*
Cake output	g/rev.	51.63 ± *1.60*	70.74 ± *0.35*
Cake + Crude oil	g/rev.	108.36 ± *1.66*	93.64 ± *0.37*
P_1	(bar)	5.27 ± *0.10*	20.60 ± *0.40*
P_2	(bar)	28.53 ± *0.22*	36.37 ± *0.22*
P_3	(bar)	38.47 ± 0.48	11.83 ± *0.13*
P_4	(bar)	59.23 ± 0.83	0.27 ± *0.05*
Temperature	(°C)	56.96 ± 0.72	57.22 ± *0.33*
Power	W	502 ± 11	689 ± *17*
SME*	Wh/kg	25.21	20.02

* *With SME = Specific Mechanical Energy* = $P/\dot{M}_{SK}$, P = Power (W); $\dot{M}_{SK}$ = flow of sunflower kernels (kg/h).

3.1.2 Solid and liquid flows

The press capacity measured as time required to process 25 kg of SK were 23.6 kg/h and 39.9 kg/h at 3.5 and 7 rpm respectively. These measurements are close to those determined as the cumulative flow rates of oil and press cakes (22.7 and 39.3 kg/h respectively, which are reported in Table 3. The discrepancies are 3.7% and 1.3%, which remain minimal and can be attributed to the differences in measurement methods. Overall, the sediment content was 18.0% at 3.5 rpm and 22.8% at 7 rpm. Oil yields, regardless of the evaluation method, differ significantly between rotational speeds, with the press at 3.5 rpm yielding approximately 2.1 times higher than at 7 rpm. This is unequivocally reflected in the residual oil content of the press cakes, which increased from 8.7% to 42.6% with the increase in rotational speed.

The screw speed largely accounts for the difference in overall flow rate; however, it may be valuable to compare these flow rates by normalizing them to the quantities produced per screw revolution. The second part of Table 3 (with grey background) shows the measured quantities of press cake and oil per revolution, as well as the production of clarified oil and the sum of crude oil and press cake. This analysis reveals that the quantities of crude and clarified oil produced per rotation are 2.48 and 2.67 times higher at low speed, respectively, while the press cake flow rate per revolution is reduced by a factor of 0.73. Overall, the press throughput per rotation at low speed was significantly higher, with a 1.16-fold increase compared to the highest speed (all differences were statistically significant; Tukey's test, $P < 0.0001$ for each variable)

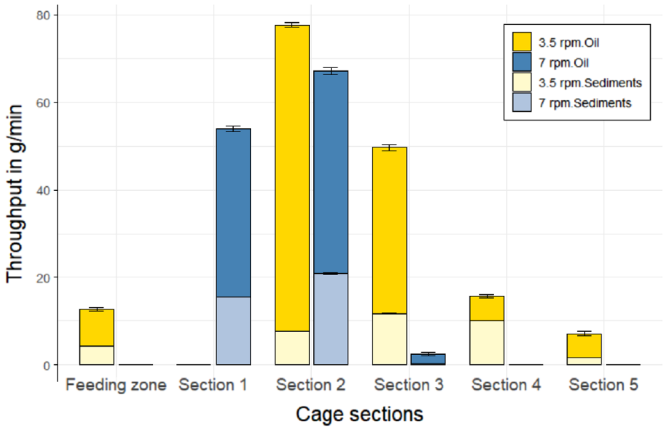

Fig. 6. Oil and sediments flow rates measured under each cage section.

Figure 6 illustrates the oil and sediment fluxes measured beneath the cage for each section defined in Figure 1. The flow rates are presented in grams per minute. At 3.5 rpm, the flow rate is characterized by a maximum in section 2, followed by a gradual decrease in sections 3 to 5. Sediment production becomes progressively more significant, although it remains relatively stable in absolute values, except for section 5. More surprising is the oil production in section 0, which is the feeding zone and does not produce compression, while no oil is produced in section 1. Comparatively, at 7 rpm, oil is first produced in section 1, then more significantly in section 2, before dropping to almost nothing in section 3 and becoming negligible in the last two sections. Sediment production is proportionally higher than at 3.5 rpm.

3.1.3 Evolution of oil content in the cake within the press

The oil extraction zones are correlated with the residual oil content in the cake measured along the press, as illustrated in Figure 7. The analysis of oil content evolution reveals a more rapid reduction at 7 rpm during the initial compression phases, with a significant decrease observed in screw 'C' when passing through ring 'D'. Subsequently, the oil content remains relatively stable in the upstream portion of screw 'E', followed by another decrease in the terminal section of this screw as it passes through cone 'F'. The oil content then increases in the upstream portion of screw 'G', returning to levels observed at the exit of screw 'E' by the time it leaves screw 'G'. This oil content, approximately 40%, is then maintained through segments 'H' to 'L'.

It is noteworthy that the two cage sections with the highest oil flow rates at 7 rpm (Sections 2 and 3) correspond to screws 'C' and 'E', where the most significant decreases in oil content are observed.

At 3.5 rpm, the oil content shows little change up to the entrance of screw 'E', which is in the vicinity of cage section 1

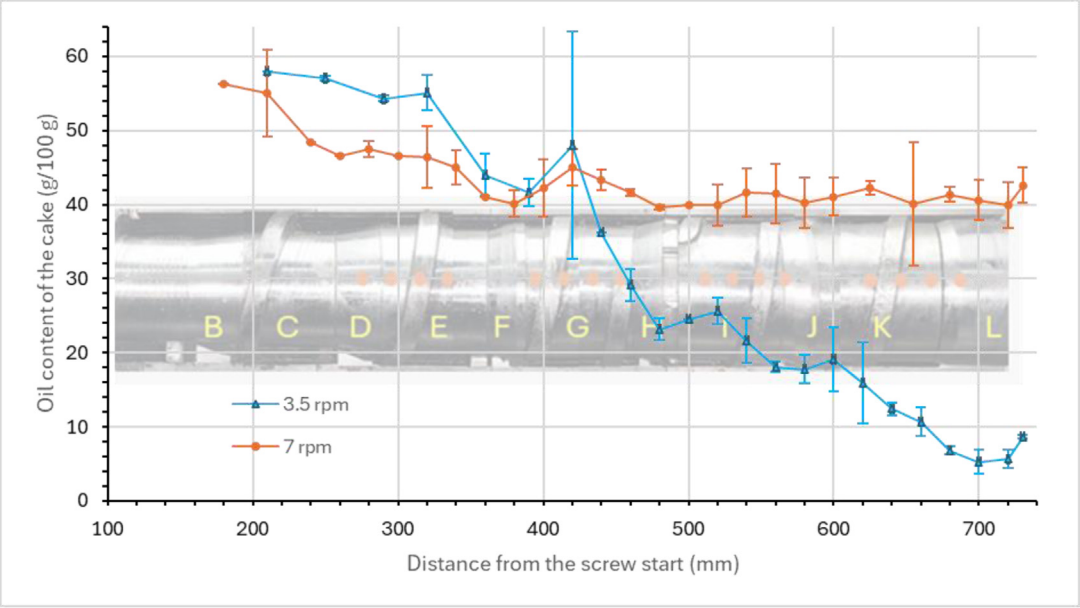

Fig. 7. Residual oil content of sunflower kernels cake into the press cage related to the rotation speed and the position of the recovery in the press cage.

Table 4. Comparison between the observed flowrates and the theoretical throughput of each screw segment.

	Screw	*i*	Volume (L/h)	Oil cont. (g/g)	Density	Potential flow (kg/h)	Solid ($\dot{S}_i$) (kg/h)	Oil (kg/h)	Total (kg/h)	Real / Pot.
3.5 rpm	**A**	1	62.13	0.57	0.58	36.03	22.75	1.02 ± 0.12	23.77	0.63
	C	2	40.22	0.57	0.58	23.33	21.73	0.00	21.73	0.93
	E	3	25.06	0.54	0.76	19.04	19.16	5.12 ± 0.14	21.73	1.01
	G	4	20.85	0.42	0.80	16.77	14.76	3.68 ± 0.17	16.60	0.88
	I	5	18.53	0.24	0.87	16.16	12.14	1.55 ± 0.11	12.92	0.75
	K	6	15.16	0.16	0.90	13.68	11.10	0.53 ± 0.13	11.37	0.81
7 rpm	**A**	1	127.44	0.57	0.58	73.92	39.32	0.00	39.32	0.53
	C	2	82.51	0.52	0.58	47.86	37.23	4.17 ± 0.08	39.32	0.78
	E	3	51.41	0.44	0.80	40.93	32.51	5.28 ± 0.10	35.15	0.79
	G	4	42.77	0.43	0.80	34.18	29.79	0.16 ± 0.06	29.87	0.87
	I	5	38.02	0.41	0.81	30.71	29.71	0.00	29.71	0.97
	K	6	31.10	0.41	0.81	25.14	29.71	0.00	29.71	1.18

Potential flow = theoretical flow transported by the screw. Solid: see hereafter. Oil: oil flow rate measured. Real/Pot. : ratio of measured flow (Solid column) to Potential flow.

that did not produce oil. The exit of screw 'E' achieves approximately the same reduction in oil content as the combined effect of screws 'C' and 'E' at 7 rpm. At the rear of screw 'G', a similar increase in oil content is observed as at 7 rpm. A very large standard deviation is observed in the first measurement point point of screw 'G' indicating a special behaviour of the material at this point. However, the terminal portion of screw 'G' produces a substantial reduction in oil content, dropping from 48% to 25% - corresponding to cage section 3 where the highest oil flow rate was observed. Passage through the cone ring 'H' is followed by a slight increase in oil content (~2%). Like with the previous screws, the most significant deoiling occurs in the last portion of screw 'I', while progression halts in the area of cone 'J'. Screw segment 'K' generates a regular decrease of the oil content up to entry of the ring 'L'. A small increase is observed in the last measured sample.

3.1.4 Cross-examination of the press flow rates and geometry

Given the flow rate data measured at the outlet of each section of the cage and the cake outlet, as well as the data related to the press screw geometry, it seems useful to compare this information to verify its consistency and attempt to draw some observations. To transition from screw geometry to flow rate considerations, it is necessary to transform the volumes generated by the screw rotation into mass flow rates of solids transported by the screw. To achieve this, we assume that the

volume of solid material that the screw can displace with each rotation corresponds to the available volume between the shaft and the cage over a length equivalent to the pitch of the screw segments. Converting from volume to flow rate requires additional information, namely the product density. This information is difficult to establish since the solid in the press is constrained by pressure, and its density under pressure is likely different from its density at atmospheric pressure. We estimated this value for cakes with different oil contents at 60°C by precisely measuring the volume occupied by a known mass of cake using a unidirectional press with a compression chamber without orifices under a pressure of 300 bars. These measurements allowed us to establish an estimate of the density according to equation (8) and use the results for assessing the potential flow of material passing through each screw segment as given in the column "Potential flow" in Table 4.

$$\rho = 0.962 - 0.376 * X_O^C, \tag{8}$$

with ρ: the density and X_O^C: the cake oil content.

Furthermore, before compression, sunflower kernels have an apparent density of 0.58.

The 'Solid' column represents the cake flow rate for the section calculated according to equation (9)

$$\dot{S}_i = \dot{S}_{i+1} + \frac{1}{2}(\dot{O}_{i+1} + \dot{O}_i), \tag{9}$$

with $\dot{S}_i$ = flow rate of solid of the screw segment i, $i \in (2, 3, 4, 5, 6)$, $\dot{S}_7$ = cake flow rate, $\dot{S}_1$ = total oil + cake flow rate. $\dot{O}_i$ = crude oil flow of segment i.

At 3.5 rpm, all the ratios real/Potential are lower than 100% except for the screw 'E" with the highest value (1,01). At 7 rpm, the highest ratio is observed in the screw segment 'K' (1,18). The ratio greater than 1 can be explained by the low flow rate of oil passing through the cage, which results in a higher flow rate of oil being transported with the cake stream.

3.2 Critical pressure of extrusion

The difference in sunflower kernel behaviour within the press at two relatively slow rotational speeds is difficult to explain solely based on data obtained from pilot-scale experiments using the MBU 20 press. Consequently, it was necessary to supplement this information with observations from a unidirectional press, which represents a less complex and more easily observable system. To this end, kernels were placed in a compression chamber, and the resistance to piston displacement was monitored for a range of piston displacement speeds between 1 and 20 mm per minute. The objective was to identify the pressure at which the curve's behaviour changes and begins to exhibit serrations (Fig. 4), indicating the expulsion of solid matter through the perforations in the plate located at the bottom of the chamber.

Figure 8 illustrates the relationship between this critical extrusion pressure and the compression speed. It reveals a non-linear correlation between these variables, indicating that as the compression speed increases, the pressure required to induce extrusion of solids decreases. This effect is more pronounced at lower speeds compared to higher speeds. This pressure is around 200 bar for plunger speeds of 2-3 mm/min, whereas at 20 mm/min, it decreases to only about 100 bar.

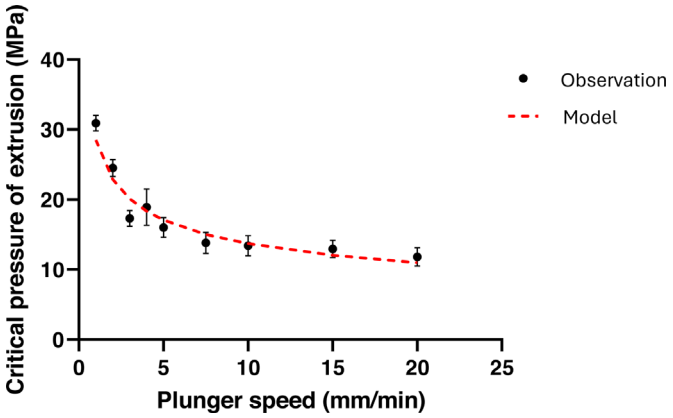

Fig. 8. Critical pressure of extrusion as a function of compression speed on sunflower kernels and the proposed model.

The decrease in critical pressure can be modelled with a simple power function ($A \times v^{-n}$, constant A = 305.8 (N mm^{-1} m^{-2}), constant n = 0.376, v the plunger speed in mm/min, R^2 = 0.967).

4 Discussions

4.1 Oil yields and rotation speed

Yields (Tab. 4). The higher speed of the screw resulted in a substantial loss of yield, regardless of the evaluation method employed (which depended on how sediments were accounted for), with ratios of 2.1 between 3.5 and 7 rpm observed across all three yield calculation methods. The minimal discrepancy between Method 1 and Method 2 is unexpected, given that the presence of sediments in the crude oil should have led to an overestimation of yield compared to the estimation based on oil content. It is therefore probable that the NMR-based oil content measurement tends to slightly underestimate the residual oil content. Chapuis *et al.* (2014) working with a similar press observed a dramatic drop in oil yields beyond 5 rpm. Other works made on Komet screw presses observed a lower rate of losses. However, Komet presses have a very simple design which is less sensitive to the issue of filtration resistance.

Oil backflow. The oil output observed at section 0 of the cage at 3.5 rpm, despite this area not producing compression, can be explained by an oil backflow towards the cage section where the gap between the bars is widest before it can flow out. This suggests that the spaces between the bars in section 1 were likely obstructed by solid material, so the low oil pressure in this area was unable to overcome. This phenomenon was described by Carré (2022), who emphasized the importance of providing sufficient spacing between the bars to maintain cage permeability. Carré indicates that when this is not the case, oil can accumulate in the feeding zone to the point of disrupting press operation.

Role of cone rings. The measure of the oil content in the press (Fig. 7) shows that the restriction given by the

presence of conical rings in the worm assembly is not associated with reductions in oil content. For cones 'F' and 'H', this phenomenon could be attributed to their location opposite clamping rings F2 and F3, where oil may encounter greater difficulty in exiting. However, this explanation does not hold for ring 'J', positioned upstream of clamping ring F4, where a similar interruption in the cake's oil content reduction is observed. Moreover, the presence of clamping rings opposite the cones does not necessarily preclude all cage porosity, as nothing impedes oil exit by the cage. These measurements are corroborated by the visual appearance of the cake at these constriction points, which appears "oilier" than in upstream and downstream zones. Given that these devices are likely to cause the most significant compression and in consequence the highest pressures, this result seems paradoxical. Our interpretation posits that the compression speed in these regions is probably excessive, resulting in oil entrapment within the matrix. We may thus speculate that this could affect the solid's rheology, causing it to soften and more readily overcome the obstacle. Also, the reabsorption of oil by the cake when the press stops can be envisaged. In fact, the high pressure at certain points returns to zero, which can encourage oil reabsorption thanks to the relaxation of the material.

Power and power variations. The specific mechanical energy (SME) in Table 3 is lower for 7 rpm than at 3.5 rpm which is not surprising knowing the lesser performance of the press in terms of oil yield, and pressure generation. The soft cake produced at 7 rpm demands less energy to be processed since it offers less resistance to the thrust of the thread of the screw.

4.2 Press geometry, flowrates and the concept of dominant screw segment

The calculation of theoretical volumes passing through each screw segment as presented in Table 4 warrants further discussion. The transported volume should account for the thread thickness, which should theoretically reduce the potentially transported volume. However, when applying this correction, the actual flow rates significantly exceed the theoretical transport capacity of the press. It is possible that the dynamic axial compression produced by the press allows for greater solid compression than what we evaluated using the unidirectional press. This discrepancy may not necessarily be due to higher pressure, but rather because when introducing the material into the unidirectional press, even under 300 bars of pressure, we may not achieve a material distribution as dense as that produced by the continuous action of the screws. The continuous, dynamic nature of the screw press may induce more efficient compaction and material distribution, potentially explaining the observed discrepancy between theoretical calculations and actual performance. The method of calculating solid flux based on the average between incoming and outgoing flows provides only a rough estimate. Indeed, incoming flow is higher than outgoing flow as the oil flows out of the press through the barrel. Nevertheless, this approach offers a general overview of each screw segment's operation, which is not without interest. Indeed, it is noteworthy that for each rotation speed, there exists a segment whose real/Potential ratio is close to 1. This section likely determines the effective flow rate of the press. For upstream sections, it constitutes the limiting factor that imposes a backflow towards the feeding zone, while for downstream sections, it imposes a potentially limiting feed rate that could result in cake decompaction in the rear part of the screw segments, favouring porosity regeneration. We propose to designate this screw segment as the "dominant segment" in order to examine the utility of this concept for analysing press operation. We observe that screw 'E' plays this role at 3.5 rpm, allowing the three downstream screws to operate with a certain efficiency. At 7 rpm, screw 'I' assumed this role and appears to impose an overfeeding on screw 'K', forcing a flow rate higher than it is supposed to generate. This is likely made possible by the plasticity of the cake, which is very rich in oil.

It is evident that the concept of a dominant screw segment cannot be attributed solely to screw geometry or raw material characteristics, as these factors remain constant across both rotational speeds. Consequently, the determinant of the dominant segment's position is intrinsically linked to the material's behaviour within the screw, particularly its oil extraction rate. At the lower rotational speed, screw segments 'G', 'I', and 'K' maintained their compressive function, effectively reducing the volume of material to be processed by downstream segments. As a result, these downstream segments were underutilized due to reduced material input from upstream. In contrast, at 7 rpm, for reasons that warrant further investigation, screw segments 'A', 'C', 'E', and 'G' are consistently forced to reject a portion of the material they should have absorbed and compressed. The phenomenon of back-flow, or reflux, is a critical aspect of screw press operation that significantly impacts extraction efficiency. This reverse movement of material within the screw channels occurs due to pressure gradients and the complex interactions between the screw geometry and the processed material (Uitterhaegen and Evon, 2017). Back-flow can lead to increased residence time and enhanced mixing, which may be beneficial for certain processes (Isobe *et al.*, 1992). However, excessive backflow can also result in reduced throughput and decreased extraction yields, particularly in low-fibre matrices such as dehulled oilseeds (Bogaert *et al.*, 2018). The balance between forward conveyance and back-flow is crucial for optimizing press performance and is influenced by factors such as screw design, rotation speed, and material properties (Kabutey *et al.*, 2017).

4.3 Critical extrusion pressure and press malfunction at higher speed

The impact of compression speed on oil extraction efficiency in screw presses has been a subject of significant research. Raß (2001) observed that increasing compression speed leads to a more rapid rise in liquid pressure within the cake, especially with dehulled material. This phenomenon can be attributed to the oil flux generating pressure that exceeds the solid material's resistance capacity. Consequently, this may result in the collapse of the capillary network through which oil flows, as suggested by Bogaert *et al.* (2018). Such collapse manifests as a sudden increase in liquid pressure and the passage of solid material through the press orifices. Carré (2022) further elaborated on this concept, noting that the absence of hulls in dehulled seeds exacerbates this effect by

reducing the cake's structural integrity. This mechanism could explain the observed decrease in press performance when processing low-fibre matrices at higher speeds, as reported by Chapuis *et al.* (2014) in their study of *Jatropha curcas* kernels.

The reduction of the critical pressure of extrusion observed on Figure 8 confirms the existence of this mechanism in sunflower kernels and is likely to explain the difference of press performance with the acceleration of the rotational speed. Our primary hypothesis posits that the observed performance decline at 7 rpm can be attributed to the heightened filtration resistance of the hull-free material. When the volume of oil to be displaced exceeds the capacity of the capillary network, a substantial increase in liquid pressure occurs, precipitating a change in the material's behaviour. This behavioural shift differs from that observed in the compression chamber of a unidirectional press. In this instance, rather than solid extrusion through the press orifices, we observe a more pronounced backflow towards the upstream sections preceding segment 'I', coupled with an acceleration of flow in segment 'K'.

At this stage of our investigation, we are unable to correlate pressure measurements from the piston press with those from the screw press. Understanding the compression speed is a critical parameter that we currently cannot assess in the screw press. If compression were solely due to changes in screw segment diameter, the rotation speed would have no effect on compression speed, as volume reduction would depend only on the press geometry. However, passing through restrictions forces the solid material to deform to overcome the obstacle and increase the flow per unit area (provided the downstream screw segment allows it). This generates pressure, which promotes compression. What we cannot estimate is the distribution of the volume displaced by the screw thread between: 1) material that successfully passes through the restriction, 2) material that fails to pass and rotates with the screw, 3) actual compression leading to oil expulsion. To further complicate matters, we must also account for imbalances between the transport capacity of the screws and the limiting effect of the dominant screw (if located upstream of the screw in question). Additionally, fluctuations in the pressure measured along the cage demonstrate that pressure is far from uniform within a screw segment, which strongly deviates from a model reducible to a series of piston presses.

5 Conclusion

This study provides significant insights into the mechanics of oil extraction from dehulled sunflower kernels using an instrumented screw press. The comprehensive experimental setup, including pressure sensors and temperature probes allowed for a detailed analysis of the pressing process, contributing to our understanding of the complex interactions between seed material properties, press geometry, and operating conditions in mechanical oil extraction of dehulled seeds. One of the most significant findings of this research is the definitive refutation of the "lack of friction" hypothesis as the primary cause of poor suitability for mechanical extraction in dehulled seeds. Instead, the results strongly support the concept of filtration resistance as the key factor affecting press performance (Raß, 2001). The study confirms that the absence of hulls leads to a rapid increase in liquid pressure during compression and a more fragile capillary network, resulting in increased filtration resistance. In addition, these results demonstrate the crucial role of hulls in stabilizing capillaries during compression, maintaining filtration capacity, and enhancing the drainage capacity of the press-cake (Bogaert *et al.*, 2018). Our observations also support the hypothesis formulated by Carré (2022) regarding the role of hulls in pressure generation within screw presses and the propensity of low-fibre cakes to flow towards the outlet. This is evidenced by the oversaturation of screw 'K' by the upstream screw in the case of the 7 rpm cake. A clear demonstration has been given that it is possible to achieve high pressures when pressing sunflower kernels without necessarily succeeding in extracting oil from the matrix. This observation challenges the conventional wisdom that higher pressure invariably leads to better oil extraction.

Future research should focus on developing mathematical models to predict pressure profiles and oil yields based on seed properties, press geometry and processing parameters like temperature, moisture content, and rotational speed. Additionally, exploring innovative screw designs that can enhance oil extraction from dehulled seeds without compromising press performance would be beneficial.

The limitations of this study include its focus on a single type of sunflower kernel and steady-state operation. Future work should consider a broader range of oilseed varieties and investigate transient phenomena and long-term press performance. Moreover, the impact of sediment recycling on press performance warrants further investigation, as it could significantly affect industrial-scale operations. In conclusion, this research provides a solid foundation for understanding the challenges associated with pressing dehulled oilseeds and offers valuable insights for improving mechanical extraction processes. By addressing the identified research areas, it may be possible to design more efficient and sustainable oil production processes, potentially reducing the need for solvent extraction and its associated environmental and safety concerns.

Acknowledgments

This work was funded by the French Ministry of Agriculture and Food as part of France Relance's protein plan, with support from Terres Univia. The project also received support from ANRT for the funding of a PhD student.

Conflicts of interest

The authors declare they have no financial interests or personal relationships that could have appeared to influence the work reported in this paper.

Author contribution statement

Florian Rousseau: conceptualization, writing original draft; Patrick Carré, conceptualization, project administration, writing, review & editing; Têko Gouyo: review & editing; Raphaëlle Savoire: conceptualization, validation, writing, review & editing.

References

Bogaert L, Mhemdi H, Vorobiev E. 2018. Impact of pretreatments on the solid/liquid expression behavior of canola seeds based on the simplified computational method. Ind Crops Prod 113: 135–141.

Canibe N, Pedrosa MM, Robredo LM, Bach Knudsen KE. 1999. Chemical composition, digestibility and protein quality of 12 sunflower (*Helianthus annuus* L) cultivars. J Sci Food Agric 79: 1775–1782.

Carré P. 2022. New approach for the elucidation of the phenomena involved in the operation of vegetable oil extraction presses. OCL 29: 6.

Carré P, Rousseau F, Gouyo T, Savoire R. 2025, Insights from an Instrumented Screw Press: Investigating pressure, torque, cage strain and flows dynamic. OCL, on press.

Chapuis A, Blin J, Carré P, Lecomte D. 2014. Separation efficiency and energy consumption of oil expression using a screw-press: the case of *Jatropha curcas* L. seeds. Ind Crops Prod 52: 752–761.

Demirel C, Kabutey A, Herak D, Gurdil GAK. 2017. Numerical estimation of deformation energy of selected bulk oilseeds in compression loading. IOP Conf Ser: Mater Sci Eng 237: 012004.

Divisova M, Herak D, Kabutey A, Sigalingging R, Svatonova T. 2014. Deformation curve characteristics of rapeseeds and sunflower seeds under compression loading. Sci Agric Bohem 45: 180–186.

INRAE-CIRAD-AFZ. 2024. Feed tables. https://www.feedtables.com

Isobe S, Zuber F, Uemura K, Noguchi A. 1992. A new twin-screw press design for oil extraction of dehulled sunflower seeds. J Am Oil Chem Soc 69: 884–889.

Kabutey A, Herák D, Chotěborský R, Sigalingging R, Mizera Č. 2015. Effect of compression speed on energy requirement and oil yield of *Jatropha curcas* L. bulk seeds under linear compression. Biosyst Eng 136: 8–13.

Lazaro E, Benjamin Y, Robert M. 2014. The effects of dehulling on physicochemical properties of seed oil and cake quality of sunflower. *Tanzania J Agric Sci* 13.

Mridula D, Barnwal P, Singh KK. 2015. Screw pressing performance of whole and dehulled flaxseed and some physicochemical characteristics of flaxseed oil. J Food Sci Technol 52: 1498–1506.

Mridula D, Saha D, Gupta RK, Bhadwal S. 2019. Oil expelling of dehulled sunflower: optimization of screw pressing parameters. J Food Process Preserv 43: e13852

Mridula D, Saha D, Gupta RK, Bhadwal S, Arora S, Kumar SR. 2020a. Oil expelling from dehulled de-skinned groundnut kernel using screw press: optimization of process parameters and physico-chemical characteristics. Int J Curr Microbiol Appl Sci 9: 1101–1115.

Mridula D, Saha D, Gupta R, Bhadwal S, Arora S, Kumar P, Kumar SR. 2020b. Oil expelling from whole and dehulled sunflower seeds: optimization of screw pressing parameters and Physico-chemical quality. IJCS 8: 4002–4009.

Park CS, Erickson DO, Fisher GR, Haugse CN. 1982. Effects of sunflower hulls on digestibility and performance by growing dairy heifers fed varying amounts of protein and fiber. J Dairy Sci 65: 52–58.

Raß M. 2001. *Zur Rheologie des biogenen Feststoffes unter Kompression am Beispiel geschälter Rapssaat* (Doctoral dissertation). Thesis Essen der Universität Gesamthochschule Essen. Available at: http://duepublico.uni-duisburg-essen.de/servlets/DerivateServlet/Derivate-10454/DissRass4.pdf.

Romuli S, Karaj S, Latif S, Müller J. 2017. Performance of mechanical co-extraction of Jatropha curcas L. kernels with rapeseed, maize or soybean with regard to oil recovery, press capacity and product quality. Ind Crops Prod 104: 81–90.

Savoire R, Lanoisellé JL, Vorobiev E. 2013. Mechanical continuous oil expression from oilseeds: a review. Food Bioprocess Technol 6: 1–16.

Schneider FH, Raß M. 1997. Trennpressen geschälter Rapssaat–Zielsetzung und verfahrenstechnische Probleme. Lipid/Fett 99: 91–98.

Shilong L, Xiefang L. 2011. Cold-pressed oil extraction of camellia seeds. In 2011 International Conference on New Technology of Agricultural (pp. 135–138). IEEE.

Sigalingging R, Herák D., Kabutey A, Dajbych O, Hrabe P, Mizera C. 2015. Application of a tangent curve mathematical model for analysis of the mechanical behaviour of sunflower bulk seeds. Int Agrophys 29.

Terres Inovia. 2024. Qualité des graines de tournesol - Récolte 2023 [Quality of sunflower seeds – 2023 harvest]. https://www.terresinovia.fr/-/fiche-qualite-des-graines-de-tournesol. Retrieved September 20, 2024

Uitterhaegen E, Evon P. 2017. Twin-screw extrusion technology for vegetable oil extraction: a review. J Food Eng 212: 190–200.

U.S. Department of Agriculture. 2024. Production - Sunflowerseed: Production, supply and distribution online (PS&D) data. Foreign Agricultural Service. Retrieved September 20, 2024, from https://fas.usda.gov/data/production/commodity/2224000

Vadke VS, Sosulski FW. 1988. Mechanics of oil expression from canola. J Am Oil Chem Soc 65: 1169–1176.

Xiao Z, Guoxiang L, Zhi L, Shaomei W. 2005. Inversion algorithm for permeability of rapeseed cake and rapeseed dehulled cake. Trans Chin Soc Agric Eng 21: 20–24.

Zheng YL, Wiesenborn DP, Tostenson K, & Kangas N. (2003). Screw pressing of whole and dehulled flaxseed for organic oil. *J. Am. Oil Chem. Soc.*, 80(10), 1039-1045.

Cite this article as: Rousseau F, Carré P, Gouyo T, Savoire R. 2025. On the difficulty of pressing hulled sunflower seeds: challenges in mechanical oil extraction. *OCL* 32: 28. https://doi.org/10.1051/ocl/2025021